

Temperature-Dependent Ammonium Removal Capacity of Biological Activated Carbon Used in a Full-Scale Drinking Water Treatment Plant

Chotiwat Jantarakasem, Ikuro Kasuga,* Futoshi Kurisu, and Hiroaki Furumai



Cite This: *Environ. Sci. Technol.* 2020, 54, 13257–13263



Read Online

ACCESS |



Metrics & More

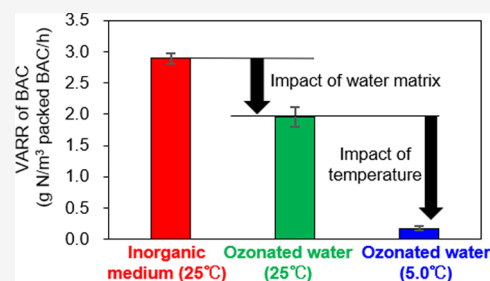


Article Recommendations



Supporting Information

ABSTRACT: Nitrification is a key function of biological activated carbon (BAC) filters for drinking water treatment. It is empirically known that the nitrification activity of BAC filters depends on water temperature, potentially resulting in the leakage of ammonium from BAC filters when the water temperature decreases. However, the ammonium removal capacity of BAC filters and factors governing the capacity remain unknown. This study employed a bench-scale column assay to determine the volumetric ammonium removal rate (VARR) of BAC collected from a full-scale drinking water treatment plant. VARR was determined at a fixed loading rate under different conditions. Seasonal variations of the VARR as well as impacts of the water matrix and water temperature on ammonium removal were quantitatively analyzed. While the VARR in an inorganic medium at 25 °C was maintained even during low water temperature periods and during breakpoint chlorination periods, the water matrix factor reduced the VARR in ozonated water at 25 °C by 33% on average. The VARR in ozonated water was dependent on water temperature, indicating that the microbial activity of BAC did not adapt to low water temperature. The Arrhenius equation was applied to reveal the relationship between VARR and water temperature. The actual ammonium removal performance of a full-scale BAC filter was predicted. VARR is useful for water engineers to reexamine the loading and filter depth of BAC filters.



1. INTRODUCTION

Ammonium poses some problems in water quality management, while it can be externally added to drinking water for chloramine disinfection.¹ The presence of ammonium in raw water not only escalates the chlorine demand in drinking water but can also lead to the formation of trichloramine, which causes the chlorine off-flavor in tap water.² Additional negative effects of residual ammonium include microbial regrowth in a distribution system based on nitrifying microorganisms³ and accumulation of nitrite due to insufficient nitrification.⁴ Biological filtration has been widely used to remove ammonium.⁵ Since 1992, the Tokyo Metropolitan Government has provided high-grade drinking water using a treatment consisting of ozonation followed by biological activated carbon (BAC) filters at all major drinking water treatment plants. Ammonia-oxidizing archaea (AOA) and ammonia-oxidizing bacteria (AOB) are involved in the rate-limiting ammonia oxidation step in biological filters including BAC.^{6–8} Recently, some microorganisms in *Nitrospira*^{9,10} have been discovered as complete ammonia oxidizers (comammox).^{11,12} Comammox is ubiquitous in biological filters for drinking water treatment.^{9,10} Since nitrification is a biological reaction performed by these microorganisms, it is highly dependent on environmental factors. For example, the nitrification activity of BAC filters can significantly deteriorate at temperatures below 10 °C.¹³ Moreover, the lack of nutrients and trace metals such as

phosphorus¹⁴ and copper^{15,16} can account for incomplete nitrification of biological sand filters. Phosphorus supplementation has been reported to partly mitigate the insufficient nitrification performance of biological sand filters.¹⁷

In practice, the ammonium removal performance of full-scale biological filters can be evaluated by simply comparing the ammonium concentrations in the influent and the effluent.¹⁸ However, accurately estimating the ammonium removal performance of biological filters is difficult, especially when the ammonium concentration in the influent is low or fluctuates. Although pilot-scale column experiments simulating full-scale treatment can determine the capacity of biological filters by manipulating the operational conditions,¹⁹ they need large footprints. Recently, a bench-scale small column assay was developed to evaluate the volumetric ammonium removal rate (VARR) of biological rapid sand filters treating groundwater.^{20,21} By applying different ammonium loading rates, the assay has been used to determine the safe operational window of rapid sand filters, which guarantees no ammonium leakage

Received: April 21, 2020

Revised: September 23, 2020

Accepted: September 24, 2020

Published: September 24, 2020



Table 1. Operational Conditions of the Bench-Scale Column Assay and Full-Scale BAC Filter Treatment

	bench-scale column assay	full-scale BAC filter
influent flow rate	109 mL/h	700 m ³ /h
influent ammonium concentration	1.0 mg NH ₄ ⁺ -N/L	<0.1 mg NH ₄ ⁺ -N/L
volumetric loading rate of ammonium	5.0 g NH ₄ ⁺ -N/m ³ packed BAC/h	<0.3 g NH ₄ ⁺ -N/m ³ packed BAC/h
hydraulic loading rate	7.0 m/h	7.0 m/h
packed BAC volume	22 cm ³	248 m ³
cross-sectional area	5.3 cm ²	99 m ²
depth of the BAC filter	4.0 cm	2.5 m
backwashing frequency		5–7 days
recirculation flow rate	3600 mL/h	

in the effluent.²⁰ Depth profiles of ammonium removal capacity of the sand filters have also been revealed.²¹ However, the impacts of the environmental factors on ammonium removal capacity have not been evaluated since the ground-water quality is very stable.

Although BAC filters are common for drinking water treatment, questions remain about the ammonium removal capacity and its dependency on environmental factors. Rarely are proactive responses made to avoid ammonium leakage from BAC filters based on information regarding the biological activity. Instead, responses are empirical. Understanding the exact capacity of biological filters is indispensable to avoid treatment failure. This study applied a bench-scale column assay to BAC used in a full-scale drinking water treatment plant to determine the seasonal variations of VARR under different conditions. By changing the condition of the column assay, we discriminated the impacts of the water matrix and water temperature on VARR. The relationship between VARR and water temperature was further investigated to evaluate ammonium removal performance of a full-scale BAC filter.

2. MATERIALS AND METHODS

2.1. Sampling. We studied a full-scale BAC filter at a drinking water treatment plant in Tokyo, Japan. Briefly, the treatment process for river water involves coagulation followed by sedimentation, ozonation, BAC filtration, and rapid sand filtration at this plant. Sodium hypochlorite is dosed after BAC filtration for disinfection, while breakpoint chlorination is implemented before coagulation to remove ammonium in the winter when the nitrification performance of BAC filters deteriorates. At this plant, breakpoint chlorination was implemented from 12 December 2018 to 3 April 2019 (average dosage: 1.6 mg Cl₂/L). Due to the deteriorated water quality, it was irregularly resumed from 12 April until 12 June 2019 (average dosage: 2.2 mg Cl₂/L). During breakpoint chlorination, ammonium in ozonated water was below the quantification limit (<0.01 mg NH₄⁺-N/L).

Sampling was performed at a specific BAC filter, which has been in service since October 2016. BAC filters were filled with AC made of coal. The effective diameter and uniformity coefficient of BAC were 1.23 mm and 1.27, respectively. The BAC filter had a cross-sectional area of 99 m² and a filter depth of 2.5 m. The average linear velocity was controlled at 7.0 m/h. Backwashing was performed at 42–48 m/h to achieve 30–40% expansion of bed depth every 5–7 days. We collected one grab sample of BAC from the center of the filter during the backwashing process using a sieve basket (30 cm × 30 cm × 30 cm). Sampling was conducted in November 2018, January, February, March, May, and June 2019. Ozonated water (influent of a BAC filter), collected on the same day of the

BAC sampling, was immediately filtrated through 0.3 μm pore size glass fiber filters (Advantec, Japan) and sterilized by an autoclave.

2.2. Batch Test. To check the adsorption of ammonium to BAC, virgin granular activated carbon (GAC) without biomass and BAC collected from the same BAC filter in June 2018 were used for the batch test. The filter material samples were incubated in an inorganic medium amended with 0.5 mg NH₄⁺-N/L of ammonium. The inorganic medium was composed of 4 mg/L KH₂PO₄, 84 mg/L NaHCO₃, 50 mg/L MgSO₄·7H₂O, 20 mg/L CaCl₂·2H₂O, and a mixture of trace elements (2.1 mg/L FeSO₄·7H₂O, 0.03 mg/L H₃BO₃, 0.1 mg/L MnCl₂·4H₂O, 0.19 mg/L CoCl₂·6H₂O, 0.024 mg/L NiCl₂·6H₂O, 0.002 mg/L CuCl₂·2H₂O, 0.144 mg/L ZnSO₄·7H₂O, and 0.036 mg/L Na₂MoO₄·2H₂O). The pH of the inorganic medium was adjusted at 7.5. GAC, or BAC (50 g wet weight) was mixed with 300 mL of the inorganic medium in a 500 mL Erlenmeyer flask in triplicate. Each flask was incubated for 8 h at 20 °C in the dark with an agitation at 72 rpm to supply air. The supernatant was collected hourly. Control experiments were performed by mixing the same amounts of GAC or BAC in Milli-Q water. To check the adsorption of nitrate on GAC, GAC (50 g wet weight) was mixed with 300 mL of the inorganic medium amended with 1.5 mg NO₃⁻-N/L of sodium nitrate in triplicate. They were incubated in the same manner as the ammonium adsorption test. Ammonium was measured by a colorimetric HACH kit (TNT830, HACH, USA). The quantification limit of the kit was 0.015 mg NH₄⁺-N/L. Nitrite and nitrate concentrations were quantified with anion ion chromatography (861 Compact IC, Metrohm, Switzerland) using a TSKgel SuperIC-Anion HS column (Tosoh Corporation, Japan). The quantification limits of nitrite and nitrate were 0.06 mg NO₂⁻-N/L and 0.05 mg NO₃⁻-N/L, respectively.

2.3. Bench-Scale Column Assay. The bench-scale column assay, which was originally developed for rapid sand filters,¹⁷ was modified to determine the VARR of BAC. Table 1 shows the experimental and full-scale operational conditions. The assay system consisted of a down-flow glass column and a tube loop with influent and effluent ports (Figure S1). The effluent of the column was recirculated with a pump (Masterflex, USA) to simulate the hydraulic loading (7.0 m/h) of a full-scale BAC filter. The high recirculation flow rate prevented stratification of the nitrification activity of the packed BAC layer.²⁰ We modified the original configuration by replacing a mixing beaker with a static mixer (N40, Noritake, Japan). The diameter and height of the column were 2.6 and 10 cm, respectively. A small amount of BAC (22 cm³) was packed in the column. The column and the static mixer were connected by a peroxide-cured silicon L/S 16 tube (Masterflex,

USA) to construct the loop line. An ammonium sulfate solution (1.0 mg $\text{NH}_4^+\text{-N/L}$) was continuously injected to the piping loop via a smooth flow pump (Q-100-VE-P-S, Tacmina, Japan) to maintain a constant volumetric ammonium loading rate (VALR) and then immediately mixed with the static mixer. Air was continuously supplied to the influent medium using an air pump. The saturated dissolved oxygen in the medium was sufficient even if 1.0 mg $\text{NH}_4^+\text{-N/L}$ was completely oxidized to nitrate. The effluent was collected from the outlet port, and the ammonium concentrations and flow rates were monitored. VALR and VARR were calculated as

$$\text{VALR} = \frac{Q_{\text{in}} C_{\text{in}}}{V_{\text{BAC}}} \quad (1)$$

$$\text{VARR} = \frac{Q_{\text{in}}(C_{\text{in}} - C_{\text{out}})}{V_{\text{BAC}}} \quad (2)$$

where VALR is the volumetric ammonium loading rate (g $\text{NH}_4^+\text{-N/m}^3$ packed BAC/h), VARR is the volumetric ammonium removal rate (g $\text{NH}_4^+\text{-N/m}^3$ packed BAC/h), Q_{in} is the influent flow rate (mL/h), C_{in} is the ammonium concentration in the influent (mg $\text{NH}_4^+\text{-N/L}$), C_{out} is the ammonium concentration in the effluent (mg $\text{NH}_4^+\text{-N/L}$), and V_{BAC} is the volume of BAC packed in the column (cm^3).

2.4. Seasonal Variations of VARR of BAC. Three different conditions were compared to determine the VARR of BAC, and all assays were performed in duplicate. BAC in the column was replaced for each assay. First, the column was operated at 25 °C with an inorganic medium amended with 1.0 mg $\text{NH}_4^+\text{-N/L}$ to estimate the VARR in the defined medium at 25 °C ($\text{VARR}_{\text{inorganic@25}}$), which corresponds to the filter media's potential of ammonium removal under the condition with no limitations or inhibitions. Second, the inorganic medium was replaced with sterilized ozonated water amended with 1.0 mg $\text{NH}_4^+\text{-N/L}$. The operational temperature was maintained at 25 °C. The VARR obtained under this condition ($\text{VARR}_{\text{ozone@25}}$) indicates the VARR of the full-scale BAC at 25 °C in the actual water matrix of ozonated water. Third, the column assay was operated using sterilized ozonated water amended with 1.0 mg $\text{NH}_4^+\text{-N/L}$ at the actual water temperature on the sampling occasion. The VARR obtained under this condition is called $\text{VARR}_{\text{ozone@T}}$. In all assays, an inorganic medium or sterilized ozonated water amended with 1.0 mg $\text{NH}_4^+\text{-N/L}$ was injected at a flow rate of 109 mL/h to maintain a volumetric ammonium loading rate of 5.0 g $\text{NH}_4^+\text{-N/m}^3$ packed BAC/h. Following preoperation for 24 h, to check stabilization of ammonium concentration in the effluent, the effluent was collected every 15 min for 4 h, and the ammonium concentrations were determined by the HACH kit.

2.5. Impact of the Water Temperature on VARR. To further study the impact of water temperature on VARR, the column assay was operated using sterilized ozonated water at different temperatures (5, 10, 15, 20, and 25 °C). BAC collected in January 2019 was used for this experiment. Sterilized ozonated water amended with 1.0 mg $\text{NH}_4^+\text{-N/L}$ was injected in the same manner as the previous experiments. Following preoperation for 24 h, the effluent samples were collected in the same manner as the previous section. The Arrhenius equation was applied to describe the temperature dependency of $\text{VARR}_{\text{ozone@T}}$ as

$$\text{VARR}_{\text{ozone@T}} = Ae^{-E/RT} \quad (3)$$

where $\text{VARR}_{\text{ozone@T}}$ is the VARR in sterilized ozonated water at temperature T (g $\text{NH}_4^+\text{-N/m}^3$ packed BAC/h), T is the temperature (K), A is the Arrhenius constant, E is the activation energy (J/mol), and R is the gas constant (8.314 J/mol/K).

The temperature activity coefficient (θ) can be calculated as

$$\text{VARR}_{\text{ozone@T2}} = \text{VARR}_{\text{ozone@T1}} \theta^{(T_2 - T_1)} \quad (4)$$

where $\theta = e^{E/(RT_1T_2)}$, and T_1 and T_2 are temperatures (K).

2.6. AOA and AOB Quantification. DNA was extracted from 0.5 g of wet BAC samples in triplicate by a Fast DNASpin kit for Soil (MP Biomedicals, USA). AOA and AOB *amoA* genes were quantified by SYBR green-based quantitative polymerase chain reaction (PCR) in triplicate with a Lightcycler 480 instrument (Roche, Switzerland). Primers Arch-*amoA*F (5'-STAATGGTCTGGCTTAGACG-3') and Arch-*amoA*R (5'-GCGGCCATCCATCTGTATGT-3') were used for AOA *amoA* genes.²² Primers *amoA*-1F* (5'-GGGGHTTYTACTGGTGGT-3') and *amoA*-2R (5'-CCCCTCKGSAAGCCTTCTTC-3') were used for AOB *amoA* genes.²³ Lightcycler 480 SYBR Green I Master (Roche, Switzerland) was used to prepare the reaction mixtures. All reaction conditions are described elsewhere.²⁴ One-way analysis of variance (ANOVA) with post-hoc Tukey's test was used to evaluate the differences in logarithmically transformed AOA and AOB abundances (SPSS 19.0, IBM, USA).

3. RESULTS AND DISCUSSION

3.1. Batch Experiment. Virgin GAC and BAC were incubated in an inorganic medium amended with ammonium to evaluate nitrification activity (Figure S2). In the control experiment using Milli-Q water, virgin GAC and BAC did not release ammonium. In an inorganic medium amended with ammonium, the ammonium adsorption capability of virgin GAC was minimal. On the other hand, BAC reduced the ammonium concentration below the quantification limit after 8 h. Hence, biological functions mostly account for the removal of ammonium in BAC. Although virgin GAC did not result in nitrate release, the nitrate concentration increased to 1.6 mg $\text{NO}_3^-\text{-N/L}$ and 1.2 mg $\text{NO}_3^-\text{-N/L}$ for BAC incubated in the inorganic medium amended with ammonium and for BAC in Milli-Q water, respectively. These results demonstrated that aged BAC might release nitrate. The difference in the nitrate concentration between the inorganic medium with ammonium and Milli-Q case was 0.38 mg $\text{NO}_3^-\text{-N/L}$, which was almost equivalent to ammonium removed during the incubation in an inorganic medium with ammonium (0.42 mg $\text{NH}_4^+\text{-N/L}$), further supporting that nitrification was the primary ammonium removal mechanism of BAC. In fact, virgin GAC had the potential to adsorb nitrate (Figure S3), which is consistent with previous studies.²⁵ It is suspected that the adsorbed nitrate was released from BAC due to changes in the equilibrium condition in the batch experiment.

3.2. VARR of BAC under Different Conditions. A bench-scale column assay was applied to determine $\text{VARR}_{\text{inorganic@25}}$, $\text{VARR}_{\text{ozone@25}}$, and $\text{VARR}_{\text{ozone@T}}$ of BAC. As $\text{VARR}_{\text{inorganic@25}}$ in the defined medium was consistently higher than that in ozonated water ($\text{VARR}_{\text{ozone@25}}$), $\text{VARR}_{\text{ozone@25}}$ was limited by the absence of the micronutrients and/or presence

of other inhibitory substances in the water matrix. The difference between $\text{VARR}_{\text{ozone@25}}$ and $\text{VARR}_{\text{ozone@T}}$ corresponds to the impact of water temperature. Examples of VALR and effluent ammonium concentration for the BAC sample collected in January 2019 are illustrated (Figure S4). The actual water temperature on the sampling occasion in January 2019 was 5.0 °C. Throughout the experiment, VALR was maintained near the designed value (5.0 g $\text{NH}_4^+\text{-N}/\text{m}^3$ packed BAC/h). The effluent ammonium concentration after a 24 h preoperation was stable under all conditions. The average ammonium concentration was reduced from 1.03 mg $\text{NH}_4^+\text{-N}/\text{L}$ to 0.41 mg $\text{NH}_4^+\text{-N}/\text{L}$ on average in the inorganic medium at 25 °C, whereas that in sterilized ozonated water at 25 °C was 0.60 mg $\text{NH}_4^+\text{-N}/\text{L}$, indicating that the water matrix of ozonated water reduced the ammonium removal performance. Upon lowering the water temperature to 5.0 °C in sterilized ozonated water, the ammonium removal was smaller than 0.05 mg $\text{NH}_4^+\text{-N}/\text{L}$. Low temperatures strongly inhibit the ammonium removal activity of BAC.¹³ The water matrix reduced $\text{VARR}_{\text{inorganic@25}}$ by 32%, and the temperature change from 25 to 5.0 °C reduced $\text{VARR}_{\text{ozone@25}}$ by 91%, which was only 6.1% of $\text{VARR}_{\text{inorganic@25}}$.

3.3. Seasonal Variations of VARR. Figure 1 shows seasonal variations of $\text{VARR}_{\text{inorganic@25}}$, $\text{VARR}_{\text{ozone@25}}$, and

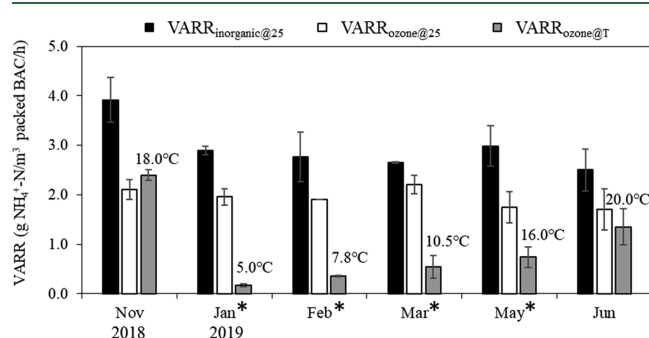


Figure 1. VARR of BAC under different conditions from November 2018 to June 2019. The water temperatures observed at the full-scale plant on the sampling occasions are shown. The same temperature conditions were applied for the assay of $\text{VARR}_{\text{ozone@T}}$. Asterisks indicate that the breakpoint chlorination was implemented on the sampling occasion. Error bars indicate the standard deviation ($n = 2$).

$\text{VARR}_{\text{ozone@T}}$ from November 2018 to June 2019. All BAC samples, except for those in November 2018 and June 2019, were collected during the breakpoint chlorination period.

$\text{VARR}_{\text{inorganic@25}}$ decreased from 3.9 g $\text{NH}_4^+\text{-N}/\text{m}^3$ packed BAC/h in November 2018 to 2.9 g $\text{NH}_4^+\text{-N}/\text{m}^3$ packed BAC/h in January 2019. However, $\text{VARR}_{\text{inorganic@25}}$ remained nearly stable (2.5–3.0 g $\text{NH}_4^+\text{-N}/\text{m}^3$ packed BAC/h) from January to June even when the water temperature gradually increased and ammonium in ozonated water was below the detection limit during breakpoint chlorination. The effluent of coagulation-sedimentation basins contained 0.01–0.20 mg Cl_2/L (average: 0.07 mg Cl_2/L) of free chlorine residual during breakpoint chlorination. The impacts of temperature, ammonium starvation, and free chlorine residual on the ammonium removal should be further studied.

$\text{VARR}_{\text{ozone@25}}$ was nearly constant throughout the period (1.7–2.2 g $\text{NH}_4^+\text{-N}/\text{m}^3$ packed BAC/h). $\text{VARR}_{\text{ozone@25}}$ was 54–83% (67% on average) of $\text{VARR}_{\text{inorganic@25}}$. This suggests that a nutrient limitation or inhibitory substances in the actual water matrix lowered the potential. Previous studies demon-

strated that nitrification of the biological filter treating groundwater was suppressed when microbially available phosphorus was below 100 $\mu\text{g PO}_4\text{-P}/\text{L}$,¹⁴ and a copper level less than 5 $\mu\text{g}/\text{L}$ was indispensable to recover the ammonium removal rate in a full-scale sand filter.¹⁵ According to the water quality survey by the Bureau of Waterworks, Tokyo Metropolitan Government in 2017, the average phosphate concentrations in raw water and finished water ($n = 12$) at the plant were 0.12 and 0.01 mg/L, respectively. Chemical coagulation effectively removed microbially available phosphorus in drinking water, possibly limiting the VARR of BAC. The copper concentrations in raw water and finished water ($n = 4$) at the plant were below the detectable limit (10 $\mu\text{g}/\text{L}$). A future study is necessary to identify the limiting or inhibitory factors in the water matrix for VARR.

$\text{VARR}_{\text{ozone@T}}$ was strongly dependent on the water temperature. As the water temperature decreased from 18.0 °C in November 2018 to 5.0 °C in January 2019, $\text{VARR}_{\text{ozone@T}}$ dropped from 2.4 g $\text{NH}_4^+\text{-N}/\text{m}^3$ packed BAC/h to 0.18 g $\text{NH}_4^+\text{-N}/\text{m}^3$ packed BAC/h. The microbial activity of BAC did not adapt to low water temperature. Then, $\text{VARR}_{\text{ozone@T}}$ gradually increased as the water temperature rose from January to June 2019. $\text{VARR}_{\text{ozone@T}}$ in June 2019 (20.0 °C) was 1.4 g $\text{NH}_4^+\text{-N}/\text{m}^3$ packed BAC/h, which was 56% of $\text{VARR}_{\text{ozone@T}}$ in November (18.0 °C). Prolonged breakpoint chlorination, which was irregularly implemented in this season, may have inhibited the recovery of $\text{VARR}_{\text{ozone@T}}$. Actual full-scale loading rates in November 2018 and June 2019 without breakpoint chlorination were only 0.02 and 0.08 g $\text{NH}_4^+\text{-N}/\text{m}^3$ packed BAC/h, respectively, while they were zero during breakpoint chlorination since no ammonium was contained in ozonated water.

3.4. Abundances of AOA and AOB Associated with BAC. The abundances of *amoA* genes of AOA and AOB associated with BAC were measured from November 2018 to June 2019. AOA *amoA* genes were 4.0×10^7 (March 2019) to 5.6×10^8 (January 2019) gene copies/g of dry BAC, while AOB *amoA* genes were 2.2×10^5 (June 2019) to 3.4×10^6 (January 2019) gene copies/g of dry BAC (Figure S5). The predominance of AOA in BAC is consistent with previous studies analyzing different BAC filters in Japan.^{7,26} The ammonium concentration in the influent of the column assay (1.0 mg $\text{NH}_4^+\text{-N}/\text{L} = 71 \mu\text{M}$ ammonium) was much higher than the half-saturation constants of pure and enriched AOA (0.13–0.69 μM ammonium).²⁷ The abundance of AOA *amoA* genes in November 2018 was significantly higher than that in March 2019 ($p < 0.05$). The highest abundance of AOA *amoA* genes was found in January 2019, and the value was significantly higher than that in March 2019 or June 2019 ($p < 0.05$). The abundances of AOB *amoA* genes in November 2018 and January 2019 were significantly higher than those in the other months ($p < 0.05$). Although prolonged breakpoint chlorination during the sampling period might have an adverse impact especially on the abundances of AOB, further validation is necessary.

The active contribution of AOA to nitrification in a similar BAC treating low concentration of ammonium was demonstrated by DNA-stable isotope probing.⁸ Assuming that only the dominant AOA contributes to ammonium removal, all AOA cells are equally active, and each AOA cell has one copy of the *amoA* gene,²⁸ the cell-specific ammonia oxidation rate was calculated by dividing $\text{VARR}_{\text{ozone@T}}$ with the number of AOA cells on BAC. The AOA cell-specific ammonia oxidation

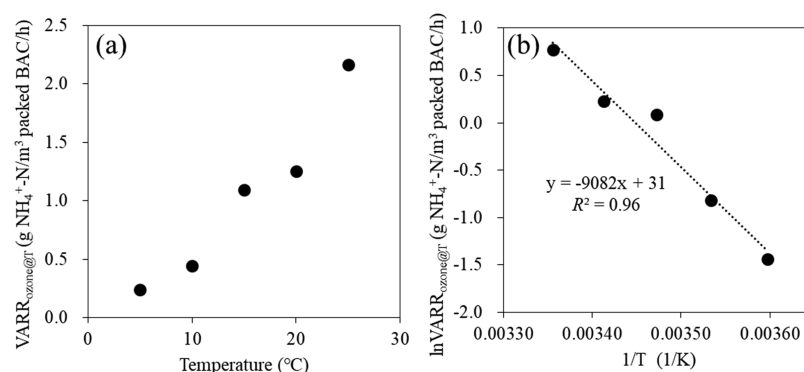


Figure 2. (a) Relationship between $\text{VARR}_{\text{ozone}@T}$ and water temperature. (b) Application of the Arrhenius equation to investigate the relationship.

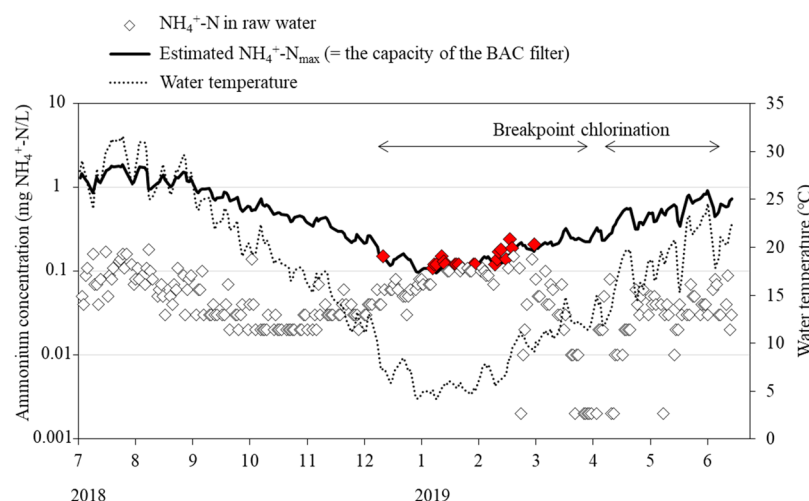


Figure 3. Relationship between ammonium in raw water and the estimated ammonium removal capacity of BAC ($\text{NH}_4^+\text{-N}_{\text{max}}$) in the full-scale BAC filter from July 2018 to June 2019. Red plots indicate that the ammonium concentration in raw water is higher than the estimated $\text{NH}_4^+\text{-N}_{\text{max}}$. The actual breakpoint chlorination period at the plant is shown by a double-headed arrow.

rates in this study were 2.0×10^{-15} , 0.04×10^{-15} , 0.36×10^{-15} , 2.0×10^{-15} , 1.1×10^{-15} , and 9.0×10^{-15} mol NH_3 oxidized/cell/h in November, January, February, March, May, and June, respectively. Based on the DNA-SIP results, the estimated cell-specific ammonia oxidation rates of AOA associated with BAC were 0.03×10^{-15} to 0.36×10^{-15} mol NH_3 oxidized/cell/h^{8,29} at 20°C in the inorganic medium supplemented with ammonium. Four marine AOA isolates demonstrated that the maximum cell-specific ammonia oxidation rates were 0.12×10^{-15} to 0.53×10^{-15} mol NH_3 oxidized/cell/h.³⁰ The estimated AOA activity in this study is almost equal to or 10 times higher than previous data. It is necessary to revisit the assumption for estimation of AOA activity including variations of gene copies. Moreover, the contributions and temperature dependency of comammox and AOB as well as AOA must be considered.

The original study using the bench-scale column assay evaluated the VARR of a biological rapid sand filter treating groundwater in Denmark.²⁰ The temperature condition was set at 10°C to match the average water temperature of groundwater, and treated water amended with ammonium was used for the assay. At a loading rate of $5.0 \text{ g } \text{NH}_4^+\text{-N}/\text{m}^3$ packed sand/h, the VARR of the sand was approximately $4\text{--}5 \text{ g } \text{NH}_4^+\text{-N}/\text{m}^3$ packed sand/h,²⁰ which was almost 10 times higher than $\text{VARR}_{\text{ozone}@T}$ in March 2019 when the water temperature was 10.5°C . Another study reported that AOB

was more abundant than or equivalent to AOA, accounting for 25–53% of the total ammonia oxidizers (AOA + AOB) in a biological rapid sand filter of the same plant in Denmark.¹⁹ The absolute abundances of AOB in the rapid sand filter (2.0×10^7 to 1.2×10^8 cell-based copies/g drain wet weight sand) were much higher than AOB associated with BAC in our study.¹⁹ The contribution of comammox *Nitrospira* spp. to ammonia removal has also been reported in rapid sand filters in Denmark.^{9,31,32} The difference of VARR in rapid sand filters in Denmark and BAC in Japan may be due to the different compositions of the ammonia-oxidizing guilds. Different conditions, including water temperature, treatment process, type of substrates (sand vs granular activated carbon), and hydraulic loading rates (4 m/h in a case study on a specific rapid sand filter in Denmark²⁰ vs $6\text{--}7 \text{ m/h}$ in BAC in Japan), can shape the unique community structures of ammonia oxidizers in each system.¹⁹

3.5. Impact of Water Temperature on VARR . To further reveal the temperature dependency of the VARR of BAC, $\text{VARR}_{\text{ozone}@T}$ values at 5 , 10 , 15 , 20 , and 25°C were analyzed for the same BAC sample collected in January 2019. Figure 2a shows the relationship between $\text{VARR}_{\text{ozone}@T}$ and temperature. $\text{VARR}_{\text{ozone}@T}$ values at 20 , 15 , 10 , and 5°C were reduced to 58 , 50 , 20 , and 11% of $\text{VARR}_{\text{ozone}@T}$ at 25°C , respectively. Figure 2b shows the relationship between \ln

($\text{VARR}_{\text{ozone}@T}$) and $1/T$. A regression line with high R^2 (0.96) was obtained.

$$\ln \text{VARR}_{\text{ozone}@T} = -9082 \frac{1}{T} + 31 \quad (5)$$

The temperature activity coefficient (θ) of BAC was estimated to be 1.12, according to eq 4, when $T_1 = 5\text{ }^\circ\text{C}$ (278 K) and $T_2 = 20\text{ }^\circ\text{C}$ (293 K). The temperature dependence of BAC nitrification is similar to AOB ($\theta = 1.172$ at $5\text{--}20\text{ }^\circ\text{C}$).³³

We estimated $\text{VARR}_{\text{ozone}@T}$ on each day from July 2018 to June 2019 by substituting the water temperature monitored at the plant into eq 5. The maximum influent treatable ammonium concentration ($\text{NH}_4^+\text{-N}_{\text{max}}$), which is within the capacity of the BAC filter, was calculated by multiplying $\text{VARR}_{\text{ozone}@T}$ with the bed volume of the BAC filter (248 m^3) divided by the average treatment flow rate ($600\text{ m}^3/\text{h}$). Figure 3 compares the ammonium concentration in raw water and the estimated $\text{NH}_4^+\text{-N}_{\text{max}}$ from July 2018 to June 2019. Ammonium would likely leak from the effluent in the BAC filter when the actual ammonium concentration in raw water exceeds the estimated $\text{NH}_4^+\text{-N}_{\text{max}}$. Since $\text{NH}_4^+\text{-N}_{\text{max}}$ or $\text{VARR}_{\text{ozone}@T}$ is a function of water temperature, $\text{NH}_4^+\text{-N}_{\text{max}}$ decreases as the water temperature decreases. $\text{NH}_4^+\text{-N}_{\text{max}}$ was tentatively below the actual ammonium concentration on 13 December 2018 ($7.3\text{ }^\circ\text{C}$), and then, it was more frequently below the actual ammonium concentration in raw water from 9 January ($5.1\text{ }^\circ\text{C}$) to 21 February 2019 ($9.5\text{ }^\circ\text{C}$).

Considering the fact that the breakpoint chlorination was implemented at the plant on 12 December 2018, the potential ammonium leakage predicted by the model was consistent with empirical responses. The switch from biological nitrification to breakpoint chlorination sometimes follows a leakage of ammonium from BAC filters. Thus, the predicted VARR can be useful to proactively avoid leakage of ammonium from BAC filters. The best combination of biological nitrification and chemical treatment can be managed by VARR prediction along with real-time monitoring of water temperature and ammonium concentration in raw water. Based on the VARR of BAC, it is also possible that loading rates can be adjusted to below the VARR by changing treatment flow rates. In this study, VARR was determined by injecting $1.0\text{ mg NH}_4^+\text{-N/L}$ to the column, which was higher than the actual concentration range. Since this may result in an overestimation of $\text{NH}_4^+\text{-N}_{\text{max}}$, the concentration dependency of VARR should be assessed to consider the application of the column assay data to full-scale operation.

3.6. Application of VARR to Design Filter Depth. The VARR of BAC is also applicable to an evidence-based design of BAC filters. One example is the design of the filter depth. The current design specifies a 2.5 m filter depth. Based on the estimated $\text{VARR}_{\text{ozone}@T}$ from July 2018 to June 2019, $\text{NH}_4^+\text{-N}_{\text{max}}$ was calculated by simply changing the filter depth from 0.5 to 5.0 m . The number of days when ammonium leakage may have occurred in the BAC filter with different depths from July 2018 to June 2019 was estimated (Figure S6). Ammonium potentially leaked from the BAC filter for 20 days in total using the default filter depth (2.5 m). Adjusting the filter depth from 0.5 to 3.9 m reduces the number of days from 68 to 0. The results suggest that ammonium removal can be theoretically achieved without breakpoint chlorination if the filter is deeper than 3.9 m . Although various factors including construction cost, increased head loss, and the stratification of ammonia

oxidizers along with the filter depth should be considered for deep filters,²¹ the filter depth of BAC can be reexamined by incorporating VARR with a biofilm model.³⁴

■ ASSOCIATED CONTENT

Supporting Information

The Supporting Information is available free of charge at <https://pubs.acs.org/doi/10.1021/acs.est.0c02502>.

Schematic configuration of a column assay, concentrations of ammonium and nitrate in the ammonium medium incubated with BAC, concentration of nitrate in the nitrate medium incubated with virgin GAC, volumetric ammonium loading rates and ammonium concentration in the column assays, AOA and AOB abundances of BAC, and the relationship between the ammonium leakage and BAC filter depth (PDF)

■ AUTHOR INFORMATION

Corresponding Author

Ikuro Kasuga – Department of Urban Engineering, School of Engineering, The University of Tokyo, Tokyo 113-8656, Japan; orcid.org/0000-0003-4392-3756; Email: kasuga@env.t.u-tokyo.ac.jp

Authors

Chotiawat Jantarakasem – Department of Urban Engineering, School of Engineering, The University of Tokyo, Tokyo 113-8656, Japan

Futoshi Kurisu – Research Center for Water Environment Technology, School of Engineering, The University of Tokyo, Tokyo 113-8656, Japan; orcid.org/0000-0003-1567-4852

Hiroaki Furumai – Research Center for Water Environment Technology, School of Engineering, The University of Tokyo, Tokyo 113-8656, Japan

Complete contact information is available at: <https://pubs.acs.org/doi/10.1021/acs.est.0c02502>

Notes

The authors declare no competing financial interest.

■ ACKNOWLEDGMENTS

This study was partially supported by a collaborative research with the Bureau of Waterworks, Tokyo Metropolitan Government.

■ REFERENCES

- (1) He, G.; Li, C.; Dong, F.; Zhang, T.; Chen, L.; Cizmas, L.; Sharma, V. K. Chloramines in a pilot-scale water distribution system: Transformation of 17β -estradiol and formation of disinfection byproducts. *Water Res.* **2016**, *106*, 41–50.
- (2) WHO Guidelines for Drinking-Water Quality: Fourth Edition; World Health Organization: Geneva, Switzerland, 2017.
- (3) Chu, C.; Lu, C.; Lee, C. Effects of inorganic nutrients on the regrowth of heterotrophic bacteria in drinking water distribution systems. *J. Environ. Manage.* **2005**, *74*, 255–263.
- (4) Wolfe, R. L.; Means, E. G., III; Davis, M. K.; Barrett, S. E. Biological nitrification in covered reservoirs containing chloraminated water. *J. AWWA* **1988**, *80*, 109–114.
- (5) Basu, O. D.; Dhawan, S.; Black, K. Applications of biofiltration in drinking water treatment - a review. *J. Chem. Technol. Biotechnol.* **2016**, *91*, 585–595.
- (6) van der Wielen, P. W. J. J.; Voost, S.; van der Kooij, D. Ammonia-oxidizing bacteria and archaea in groundwater treatment

and drinking water distribution systems. *Appl. Environ. Microbiol.* **2009**, *75*, 4687–4695.

(7) Kasuga, I.; Nakagaki, H.; Kurisu, F.; Furumai, H. Predominance of ammonia-oxidizing archaea on granular activated carbon used in a full-scale advanced drinking water treatment plant. *Water Res.* **2010**, *44*, 5039–5049.

(8) Niu, J.; Kasuga, I.; Kurisu, F.; Furumai, H.; Shigeeda, T. Evaluation of autotrophic growth of ammonia-oxidizers associated with granular activated carbon used for drinking water purification by DNA-stable isotope probing. *Water Res.* **2013**, *47*, 7053–7065.

(9) Tatari, K.; Musovic, S.; Gülay, A.; Dechesne, A.; Albrechtsen, H.-J.; Smets, B. F. Density and distribution of nitrifying guilds in rapid sand filters for drinking water production: Dominance of *Nitrospira* spp. *Water Res.* **2017**, *127*, 239–248.

(10) Wang, Y.; Ma, L.; Mao, Y.; Jiang, X.; Xia, Y.; Yu, K.; Li, B.; Zhang, T. Comammox in drinking water systems. *Water Res.* **2017**, *116*, 332–341.

(11) Daims, H.; Lebedeva, E. V.; Pjevac, P.; Han, P.; Herbold, C.; Albertsen, M.; Jehmlich, N.; Palatinszky, M.; Vierheilig, J.; Bulaev, A.; Kirkegaard, R. H.; von Bergen, M.; Rattei, T.; Bendinger, B.; Nielsen, P. H.; Wagner, M. Complete nitrification by *Nitrospira* bacteria. *Nature* **2015**, *528*, 504–509.

(12) van Kessel, M. A. H. J.; Speth, D. R.; Albertsen, M.; Nielsen, P. H.; Op den Camp, H. J. M.; Kartal, B.; Jetten, M. S. M.; Lüscher, S. Complete nitrification by a single microorganism. *Nature* **2015**, *528*, 555–559.

(13) Andersson, A.; Laurent, P.; Kihn, A.; Prévost, M.; Servais, P. Impact of temperature on nitrification in biological activated carbon (BAC) filters used for drinking water treatment. *Water Res.* **2001**, *35*, 2923–2934.

(14) de Vet, W. W. J. M.; van Loosdrecht, M. C. M.; Rietveld, L. C. Phosphorus limitation in nitrifying groundwater filters. *Water Res.* **2012**, *46*, 1061–1069.

(15) Wagner, F. B.; Nielsen, P. B.; Boe-Hansen, R.; Albrechtsen, H.-J. Copper deficiency can limit nitrification in biological rapid sand filters for drinking water production. *Water Res.* **2016**, *95*, 280–288.

(16) Wagner, F. B.; Nielsen, P. B.; Boe-Hansen, R.; Albrechtsen, H. J. Remediation of incomplete nitrification and capacity increase of biofilters at different drinking water treatment plants through copper dosing. *Water Res.* **2018**, *132*, 42–51.

(17) van der Aa, L. T. J.; Kors, L. J.; Wind, A. P. M.; Hofman, J. A. M. H.; Rietveld, L. C. Nitrification in rapid sand filter: phosphate limitation at low temperatures. *Water Supply* **2002**, *2*, 37–46.

(18) de Vet, W. W. J. M.; Kleerebezem, R.; van der Wielen, P. W. J. J.; Rietveld, L. C.; van Loosdrecht, M. C. M. Assessment of nitrification in groundwater filters for drinking water production by qPCR and activity measurement. *Water Res.* **2011**, *45*, 4008–4018.

(19) Lee, C. O.; Boe-Hansen, R.; Musovic, S.; Smets, B.; Albrechtsen, H. J.; Binning, P. Effects of dynamic operating conditions on nitrification in biological rapid sand filters for drinking water treatment. *Water Res.* **2014**, *64*, 226–236.

(20) Tatari, K.; Smets, B. F.; Albrechtsen, H.-J. A novel bench-scale column assay to investigate site-specific nitrification biokinetics in biological rapid sand filters. *Water Res.* **2013**, *47*, 6380–6387.

(21) Tatari, K.; Smets, B. F.; Albrechtsen, H.-J. Depth investigation of rapid sand filters for drinking water production reveals strong stratification in nitrification biokinetic behavior. *Water Res.* **2016**, *101*, 402–410.

(22) Francis, C. A.; Roberts, K. J.; Beman, J. M.; Santoro, A. E.; Oakley, B. B. Ubiquity and diversity of ammonia-oxidizing archaea in water columns and sediments of the ocean. *Proc. Natl. Acad. Sci. U. S. A.* **2005**, *102*, 14683–14688.

(23) Stephen, J. R.; Chang, Y.-J.; Macnaughton, S. J.; Kowalchuk, G. A.; Leung, K. T.; Flemming, C. A.; White, D. C. Effect of toxic metals on indigenous soil beta-subgroup proteobacterium ammonia oxidizer community structure and protection against toxicity by inoculated metal-resistant bacteria. *Appl. Environ. Microbiol.* **1999**, *65*, 95–101.

(24) Kasuga, I.; Nakagaki, H.; Kurisu, F.; Furumai, H. Abundance and diversity of ammonia-oxidizing archaea and bacteria on biological

activated carbon in a pilot-scale drinking water treatment plant with different treatment processes. *Water Sci. Technol.* **2010**, *61*, 3070–3077.

(25) Moşneag, S. C.; Popescu, V.; Dinescu, A.; Borodi, G. Utilization of granular activated carbon adsorber for nitrates removal from groundwater of the Cluj region. *J. Environ. Sci. Health, Part A: Toxic/Hazard. Subst. Environ. Eng.* **2013**, *48*, 918–924.

(26) Niu, J.; Kasuga, I.; Kurisu, F.; Furumai, H.; Shigeeda, T.; Takahashi, K. Abundance and diversity of ammonia-oxidizing archaea and bacteria on granular activated carbon and their fates during drinking water purification process. *Appl. Microbiol. Biotechnol.* **2016**, *100*, 729–742.

(27) Ouyang, Y.; Norton, J. M.; Stark, J. M. Ammonium availability and temperature control contributions of ammonia oxidizing bacteria and archaea to nitrification in an agricultural soil. *Soil Biol. Biochem.* **2017**, *113*, 161–172.

(28) Alves, R. J. E.; Minh, B. Q.; Urich, T.; von Haeseler, A.; Schleper, C. Unifying the global phylogeny and environmental distribution of ammonia-oxidizing archaea based on *amoA* genes. *Nat. Commun.* **2018**, *9*, 1517.

(29) Niu, J.; Kasuga, I.; Kurisu, F.; Furumai, H. Growth competition between ammonia-oxidizing archaea and bacteria for ammonium and urea in a biological activated carbon filter used for drinking water treatment. *Environ. Sci.: Water Res. Technol.* **2019**, *5*, 231–238.

(30) Qin, W.; Heal, K. R.; Ramdasi, R.; Kobelt, J. N.; Martens-Habbena, W.; Bertagnolli, A. D.; Amin, S. A.; Walker, C. B.; Urakawa, H.; Könneke, M.; Devol, A. H.; Moffett, J. W.; Armbrust, E. V.; Jensen, G. J.; Ingalls, A. E.; Stahl, D. A. *Nitrosopumilus maritimus* gen. nov., sp. nov., *Nitrosopumilus cobalaminigenes* sp. nov., *Nitrosopumilus oxycilinae* sp. nov., and *Nitrosopumilus urephilus* sp. nov., four marine ammonia-oxidizing archaea of the phylum Thaumarchaeota. *Int. J. Syst. Evol. Microbiol.* **2017**, *67*, 5067–5079.

(31) Gülay, A.; Fowler, S. J.; Tatari, K.; Thamdrup, B.; Albrechtsen, H.-J.; Al-Soud, W. A.; Sørensen, S. J.; Smets, B. F. DNA- and RNA-SIP reveal *Nitrospira* spp. as key drivers of nitrification in groundwater-fed biofilters. *MBio* **2019**, *10*, No. e01870.

(32) Palomo, A.; Fowler, S. J.; Gülay, A.; Rasmussen, S.; Sicheritz-Ponten, T.; Smets, B. F. Metagenomic analysis of rapid gravity sand filter microbial communities suggests novel physiology of *Nitrospira* spp. *ISME J.* **2016**, *10*, 2569–2581.

(33) Guo, J.; Peng, Y.; Huang, H.; Wang, S.; Ge, S.; Zhang, J.; Wang, Z. Short- and long-term effects of temperature on partial nitrification in a sequencing batch reactor treating domestic wastewater. *J. Hazard. Mater.* **2010**, *179*, 471–479.

(34) Reichert, P. AQUASIM – A Tool for simulation and data analysis of aquatic systems. *Water Sci. Technol.* **1994**, *30*, 21–30.